Video Article

The Fibular Nerve Injury Method: A Reliable Assay to Identify and Test Factors That Repair Neuromuscular Junctions

William Dalkin[1,2], Thomas Taetzsch[1], Gregorio Valdez[1,2,3]

[1]Carilion Research Institute, Virginia Tech

[2]Carilion School of Medicine, Virginia Tech

[3]Department of Biological Sciences, Virginia Tech

Correspondence to: Gregorio Valdez at gvaldez1@vtc.vt.edu

URL: https://www.jove.com/video/54186
DOI: doi:10.3791/54186

Keywords: Neuroscience, Issue 114, NNJ, Synapse, Repair, Nerve Injury, Nerve Regeneration, Degeneration, Fibular Nerve, Peroneal Nerve, EDL

Date Published: 8/11/2016

Citation: Dalkin, W., Taetzsch, T., Valdez, G. The Fibular Nerve Injury Method: A Reliable Assay to Identify and Test Factors That Repair Neuromuscular Junctions. *J. Vis. Exp.* (114), e54186, doi:10.3791/54186 (2016).

Abstract

The neuromuscular junction (NMJ) undergoes deleterious structural and functional changes as a result of aging, injury and disease. Thus, it is imperative to understand the cellular and molecular changes involved in maintaining and repairing NMJs. For this purpose, we have developed a method to reliably and consistently examine regenerating NMJs in mice. This nerve injury method involves crushing the common fibular nerve as it passes over the lateral head of the gastrocnemius muscle tendon near the knee. Using 70 day old female mice, we demonstrate that motor axons begin to reinnervate previous postsynaptic targets within 7 days post-crush. They completely reoccupy their previous synaptic areas by 12 days. To determine the reliability of this injury method, we compared reinnervation rates between individual 70 day old female mice. We found that the number of reinnervated postsynaptic sites was similar between mice at 7, 9, and 12 days post-crush. To determine if this injury assay can also be used to compare molecular changes in muscles, we examined levels of the gamma-subunit of the muscle nicotinic receptor (gamma-AChR) and the muscle-specific kinase (MuSK). The gamma-AChR subunit and MuSK to are highly upregulated following denervation and return to normal levels following reinnervation of NMJs. We found a close relationship between transcript levels for these genes and innervation status of muscles. We believe that this method will accelerate our understanding of the cellular and molecular changes involved in repairing the NMJ and other synapses.

Video Link

The video component of this article can be found at https://www.jove.com/video/54186/

Introduction

In young adult and healthy animals, the neuromuscular junction (NMJ) is a highly stable connection between the presynapse, the nerve ending of an α-motor axon, and the postsynapse, the specialized region of an extrafusal muscle fiber where nicotinic acetylcholine receptors (AChRs) selectively aggregate[1]. The nearly perfect apposition of the pre- and post-synaptic apparatuses is necessary for proper neurotransmission, survival of α-motor neurons and muscle fibers and motor function. Unfortunately, the function of the NMJ is adversely affected by aging, diseases such as amyotrophic lateral sclerosis (ALS), autoimmune diseases and injury to muscles and peripheral nerves[2-5]. These insults often result in degeneration of presynaptic nerve endings, leaving muscles denervated and significantly altering motor skills. For this reason, the identification of molecules that function to maintain and repair the NMJ has become a priority. Because peripheral nerves regenerate and reinnervate targets, peripheral nerve injury models have been used to identify molecular changes associated with regenerating NMJs.

Peripheral nerve injury models often involve either completely cutting or crushing specific nerve branches[6]. Following a cut, the endoneurial tube has to be reformed, delaying axonal regeneration and reinnervation of target cells and tissues. The severity of this type of injury also causes axons to meander away from their original path, resulting in their failure to reach original targets. This is in contrast to nerves injured via crush where the endoneurium remains contiguous, providing a path for efficient and proper regrowth of regenerating axons. It also allows axons to find and reinnervate their original muscle fiber partners. Irrespective of injury model, there are a number of cellular and molecular changes that must occur for axons to regenerate and reinnervate targets. After an injury, the nerve segment proximal to the target is broken down and removed via a process termed Wallerian Degeneration[7]. This process involves reprogramming and de-differentiation of Schwann cells into non-myelinating cells that secrete regenerative factors, clear myelin, and recruit macrophages to the site of injury[8]. Macrophages in turn complete the clearance of myelin and axonal debris, which would otherwise impede growth of the regenerating axon[9]. In parallel, motor and sensory neurons activate mechanisms needed to promote regeneration of their severed axons. Once the regenerating axon reaches the target, it must transform from a growth cone to a nerve ending capable of properly transmitting (for motor axons) or receiving (for sensory axons) information[10]. In this regard, alpha-motor axons undergo a series of well-orchestrated changes that culminate in their growth cone differentiating into a fully functional presynaptic nerve ending that nearly perfectly opposes the post-synaptic site on the target muscle fiber[11].

The sciatic, tibial and accessory nerves have been the primary choices for studying axonal and NMJ regeneration[12-14]. However, there are a number of drawbacks when using these models to examine cellular and molecular changes associated with regenerating NMJs between animals

and under different conditions. Firstly, the sciatic nerve supplies the majority of the muscles of the hind limb, with injury significantly limiting both movement and sensation. It is therefore not possible to use this method to study the impact of exercise alone or in combination with other factors. Additionally, the sciatic nerve is a rather thick structure and thus requires a large amount of compressive force to fully injure all axons. This in turn may result in complete transection of the more superficial axons while leaving the endoneurial tube of deeper lying axons intact, introducing significant variability in the rate and fidelity of regeneration among these axons. Complete transection of this nerve is even less desirable given that many axons will fail to reconnect with the same muscle fibers. Complicating matters, the sciatic nerve possesses intrinsic anatomic variability, both in the number and site of origin of its terminal nerve branches. It is therefore very difficult to lesion the same site. While the tibial nerve is smaller and more amenable to crush injuries, there is also no readily available landmark to serve as a lesion site for this nerve branch.

The accessory nerve branch (part of cranial nerve XI) that supplies the sternocleidomastoid muscle has also been used to study regeneration of NMJs[15]. This nerve is particularly attractive because NMJs in the sternocleidomastoid muscle can be more readily imaged in live animals compared to NMJs in other muscles. But similar to the sciatic and tibial nerves, there is no specific landmark that can be used to injure this nerve in the same location, limiting it as a model for comparing regeneration of NMJs among individual animals of an experimental cohort. An inconsistent lesion site introduces variability in the rates of NMJ reinnervation. Due to these shortcomings, the procedure presented here utilizes the injury of a different peripheral nerve branch to examine regenerating NMJs.

The common fibular nerve, also called the common peroneal nerve, contains many features that make it a reliable nerve to examine regeneration of NMJs between animals and across different treatments. The common fibular nerve has a predictable anatomic course as it runs over the tendon of the lateral head of the gastrocnemius muscle in the knee, the intersection serving as a stable landmark for lesions. The nerve is accessed through a small and minimally invasive incision near but anatomically segregated from the muscles of interest. The findings presented here demonstrate that regenerating motor axons begin to reform NMJs in the extensor digitorum longus (EDL) muscle 8 days after crushing the fibular nerve in 70 days old young adult female mice. Importantly, the pattern and rate of reinnervation is consistent among animals of the same age and sex and therefore provide a reliable injury model that will significantly hasten our understanding of the cellular and molecular changes required to maintain and repair NMJs.

Protocol

All experiments were carried out under NIH guidelines and animal protocols approved by the Virginia Tech Institutional Animal Care and Use Committee.

1. Preparing Animals for Surgery

1. Anesthetize mice with a mixture of ketamine (90 mg/kg) and xylazine (10 mg/kg) via subcutaneous inguinal injection with a sterile 1 ml insulin syringe. Carrier solution contains a mixture of 0.9% saline, 17.4 mg/ml ketamine, and 2.6 mg/ml xylazine. Place animals back in cages while waiting for medication to take effect.
   NOTE: If the loading dose does not provide sufficient anesthesia for the duration of the procedure, an additional 25% of the loading dose may be injected.
2. Monitor animals post injection to check for steady respiratory rates and appropriate depression of arousal levels. Check arousal level with a hind foot pinch, which should elicit no response when sufficiently anesthetized.
   NOTE: This usually takes 3-5 min for a young adult mouse averaging 25 to 30 g. If the animal is still responsive after 10 min post injection, an additional 25% of the anesthetic loading dose may be injected.
3. Apply petrolatum and light mineral oil ophthalmic ointment to the animal's eyes to prevent dryness. Remove animals from cage and place on a clean, flat surface. Shave the desired hind limb from foot to pelvis using an electric hair trimmer, exposing only the lateral aspect of the limb.
4. Apply a chemical hair remover to the shaved site for 1 min. Manually remove the hair using laboratory wipes. Clean the depilated area with laboratory wipe soaked in ethanol.

2. Surgical Procedure

1. Sterilize surgical instruments via autoclave or other appropriate method. Clean the surgical site and surgical board with 80% ethanol/H_20. Disinfect the surgical site with proviodine. Place mouse on surgical board and align with limb restraints. Keep the target hind limb in an anatomically natural position with the knee joint slightly extended without internal or external rotation.
2. Place animal and board under the surgical microscope. Orient to the proper incision site via palpation of superficial landmarks, specifically the bony knee joint and the ridge between the tibialis anterior and gastrocnemius muscles.
3. Make an approximately 3 cm incision through the skin using a scalpel or spring scissors while using general forceps for gripping. Make the incision perpendicular to the underlying course of the common fibular nerve.
4. Continue the incision through the superficial fascia, exposing the biceps femoris and vastus lateralis muscles. Separate these muscles by cutting through the connecting deep fascia. A 1-2 cm cut should be sufficient.
5. Retract the biceps femoris muscle caudally using mechanical retractors, revealing the common fibular nerve.
6. Trace the nerve proximally until its intersection with the tendon of the lateral head of the gastrocnemius muscle is found. Note: Exposure may require additional manipulation of the retracted skin and muscle. This intersection is used as the stable landmark for the nerve injury.
7. Grasp the nerve with a fine forceps, aligning the tips in a parallel fashion to the lateral border of the gastrocnemius tendon. Crush the common fibular nerve by applying steady, hard pressure for 5 sec.
8. Corroborate full crush of the nerve by visual inspection through the surgical scope. It will appear translucent at the site of injury. If using mice expressing fluorescence proteins in peripheral axons, the fluorescence will disappear from the site of injury.
9. Remove retractors and realign muscles in their anatomic positions. Close the incision site with 6-0 silk sutures. 1-3 simple interrupted sutures is sufficient. Place recuperating mouse on a heating pad in a clean cage.

10. Monitor all animals for 2 hr post-operation to check for breathing and any adverse reactions to the anesthesia. Administer an initial dose of buprenorphine 0.05-0.10 mg/kg via subcutaneous inguinal injection immediately following recovery from surgery. Give 3 additional doses every 12 hr over the next 48 hr. After full recovery, return mice to the animal care facility.

3. Isolation and Staining of Extensor Digitorum Longus (EDL) Muscles

1. Sacrifice animals using isoflurane. Dispense 0.5 ml liquid isoflurane into a 50 ml tube packed with absorbent labwipes. Place the uncapped tube with the animal in a sealed 2,500 cm^3 chamber. At least 4 min of exposure is sufficient. Test for loss of bilateral palpebral, toe-pinch, and tail-pinch reflexes to ensure that each animal is unconscious before proceeding with perfusion.
2. Transcardially perfuse[16] animals first with 10 ml 0.1M PBS, then 25 ml of 4% paraformaldehyde in 0.1M PBS (pH 7.4). Heparin (30 units/20 g animal weight) may be added with the PBS (10 units/ml) to prevent blood clotting in small capillary beds, improving perfusion results.
3. Remove the skin covering hind limbs by using scissors to cut transversally through the skin around the circumference of the abdomen. Peel down the skin past the hind limbs and feet using forceps.
4. Remove superficial fascia of hind limbs by grasping and peeling with forceps. If using mice expressing fluorescence proteins in peripheral axons, post-fix whole mice overnight in 4% PFA in 50 ml tubes. Rinse three times with PBS.
   NOTE: Fixed mice can be stored in PBS at 4 °C. If not, skip this step and proceed to step 3.6 without post-fixing animals.
5. Dissect out EDL muscles[18] from mouse hind limbs, being sure to keep proximal and distal tendons as intact as possible.
6. Incubate EDL muscles in blocking buffer (1x PBS containing 0.5% Triton X-100, 3% BSA and 5% goat serum) for at least 1 hr.
7. To visualize motor axons and their nerve terminals, place muscles in tubes containing neurofilament (1:1,000) and synaptotagmin-2 (1:250) antibodies diluted in blocking buffer for 3 days. Wash muscles three times with 1x PBS and 10 min each time. Note: Skip this step if using mice expressing fluorescence proteins (XFP) in peripheral axons.
8. Stain the contralateral uninjured EDL as a positive control for complete NMJ innervation. Negative controls should include an EDL obtained at 4 days post-injury, a time point where the NMJ is completely denervated, as well as an EDL stained with secondary antibody only.
9. Incubate muscles with appropriate fluorescently tagged secondary antibodies to detect neurofilament and synaptotagmin-2 for 1 day. Wash muscles three times with 1x PBS and 10 min each time. Note: This step can be carried out together with step 3.10. Skip this step if using mice expressing fluorescence proteins in peripheral axons.
10. To visualize the postsynaptic region of the NMJ, incubate muscles with 5 µg/ml Alexa-555 conjugated alpha-bungarotoxin diluted in blocking buffer for at least 2 hr. Wash muscles three times with 1x PBS and 10 min each time.
11. To mount whole muscles on positively charged glass slides, place the muscle directly on the slide, add a few drops of glycerol based mounting medium on the slide and cover with a coverslip. Press the coverslip against the slide to flatten the muscle. Soak off mounting media from the perimeter of the slide and coverslip using laboratory wipes. Apply nail polish to seal the edges between the coverslip and slide.

4. Imaging and Data Analysis

1. To analyze the structure of NMJs, image the EDL muscle using a confocal laser scanning microscope equipped to excite 488, 555 and 633 nm light and capture the emitted light with 20X and 40X objectives.
2. To visualize whole NMJs, create maximum intensity projection images of optical sections spaced 1 to 2 µm apart extending from the lowest to highest visible regions of the NMJ. Create maximum intensity projections using commercially available imaging software.
3. To determine rates of reinnervation, categorize NMJs as: 1) completely denervated = postsynaptic site is completely devoid of contact with axon, less than 5% colocalization between the axon and AChRs. 2) Partially innervated = the axon partially overlaps the postsynapse, 5-95% colocalization between the axon and AChRs. 3) Full innervation = nearly perfect apposition between the pre- and post-synapse, greater than 95% colocalization between the axon and AChRs. Exclude NMJs that lie perpendicular to the imaging plane or are not fully visualized in the image. Note: In all these experiments, at least 3 animals and 50 NMJs per animal were examined. Results were deemed significant using a student t-test with a P value of less than 0.05.
4. To blind the operator, separate individuals can perform the surgery and image analysis. Without knowledge of the treatment groups, the analyzer can be objective with NMJ scoring. Alternatively, images can be randomized and presented to the operator for analysis without knowledge of the source animal.

5. Quantitative PCR

1. Sacrifice animals using isoflurane and cervical dislocation. Remove skin and superficial fascia covering leg muscles according to step 3.3. Dissect tibialis anterior and EDL muscles according to step 3.4.
2. Flash freeze the entire tibialis anterior and EDL muscles in a 1.5 ml tube over liquid nitrogen. Remove tissue from tube and place in a pre-chilled mortar partially submerged in liquid nitrogen. Grind frozen muscle into a fine powder using a mortar and pestle.
3. Dissolve frozen muscle powder into a commercially available RNA extraction reagent and perform RNA extraction and genomic DNA removal with a commercially available kit according to manufacturer's instructions.
4. Perform reverse transcription with a commercially available reverse transcriptase mix according to manufacturer's instructions.
5. Perform qPCR using a commercially available kit using appropriate housekeeping genes (see table of materials). Use a commercially available quantitative PCR thermal cycler to carry out PCR (see table of materials).
6. Set annealing temperature to 58 °C. Adjust additional cycling parameters to specifications of the manufacturer of taq polymerase/SYBR green mix. Include a final melt curve step in thermal cycler program consisting of 0.5 °C incremental increases from 65 °C to 95 °C to test for primer specificity and primer dimer formation.
7. Determine relative mRNA expression levels by the $2^{-\Delta\Delta CT}$ method[21] using 18S RNA as the control gene.

Representative Results

The common fibular nerve, also called the common peroneal nerve, arises from the sciatic nerve above the popliteal fossa, where it swings around the head of the fibula to the anterior aspect of the leg (**Figure 1A**). There it branches into the superficial and deep fibular nerves, together supplying the dorsiflexors of the foot and toes (anterior tibialis, extensor digitorum longus and brevis, and extensor halluces longus muscles), and the everters of the foot (peroneus muscles). This nerve also carries sensory fibers that project to the dorsum of the foot and lateral aspect of the lower half of the leg. It is a relatively thin structure composed of motor and sensory axons. This nerve branch follows a predictable anatomic course. Lateral to the knee, the nerve is mostly superficial as it runs over the tendon of the lateral head of the gastrocnemius muscle (**Figure 1** and **Figure 2**). This location serves as a stable landmark that can be easily reached with a small incision, limiting damage to skin and fascia (**Figure 1A**). The smaller diameter of this nerve, when compared to the sciatic and tibial nerves, makes it possible to crush all axons using less force, reducing the likelihood of completely severing the more superficial axons.

Mice expressing yellow fluorescence protein (YFP) only in neurons[17] were used to optimize the crush procedure on the common fibular nerve and unambiguously visualize regenerating axons. The nerve was crushed at the edge of the gastrocnemius tendon most proximal to the target muscles because this site is more accessible from the location of the incision. This site also serves as a reliable anatomical landmark, making it possible to compare regeneration of NMJs among animals of the same age and sex. Compressing the nerve for 5 sec using a fine forceps results in the disappearance of YFP from the site of injury (**Figure 2B**). However, the connective tissue and cells residing in the epineurium remain contiguous, serving as a conduit for rapid and precise regeneration of axons to their original targets (**Figure 2B**). In 70 days old female mice, this injury is sufficient to cause degeneration of all axonal segments distal from the neuronal soma (**Figure 4B**).

To determine the reliability and reproducibility of this injury method, reinnervation of the extensor digitorum longus (EDL) muscle was examined. This muscle was chosen for several reasons: 1) It is proximal yet physically separated from the incision and nerve injury sites (**Figure 3A**). Hence, the muscle is only altered by degeneration of severed innervating axons. Its proximity to the crush site minimizes the time needed for it to be reinnervated and muscle atrophy. 2) It is primarily composed of fast type skeletal muscle fibers, which are more susceptible to aging and diseases. 3) Its NMJs undergo significant structural changes during the progression of diseases and aging that can be attenuated by exercise and caloric restriction. 4) It is readily accessible for live imaging and molecular manipulation (**Figure 3D**). 5) It can be easily separated into its four phalangeal components that can be whole-mounted making it possible to fully image all of its innervating axons and their connections using light microscopy (**Figure 3B**).

Reinnervation of previously vacated post-synaptic sites after crushing the fibular nerve on the right leg was assessed in three 70 days old female mice expressing YFP in motor axons. Post-synaptic sites were visualized using fluorescently tagged alpha-bungarotoxin (BTX), which binds selectively and with high affinity to muscles nAChRs. Muscles were deemed to be denervated, partially or fully reinnervated following these criteria: 1) In denervated muscle fibers, motor axons were completely missing from post-synaptic sites and less than 5% colocalization between the axon and AChRs was observed. 2) Partially innervated muscle fibers were categorized by some but incomplete apposition of motor axons with post-synaptic sites and 5-95% colocalization between the axon and AChRs was observed. 3) In fully innervated muscle fibers, there was nearly perfect apposition between motor nerve endings and post-synaptic sites and greater than 95% colocalization between the axon and AChRs was observed. Individual NMJs were excluded from counts if their endplates lay perpendicular to the imaging plane or the whole NMJ was not visualized. Using these criteria, high concordance in the rate and degree of reinnervation was observed among all mice examined. At 4 days post-crush, muscles were found completely denervated in all animals examined (**Figure 4B**). This finding shows that crushing the common fibular nerve for 5 sec, as described above, is sufficient to sever all axons. By 7 days post-crush, nerve endings were in the process of reoccupying previously vacated post-synaptic sites (**Figure 4C**, **4E-F**). However, most muscle fibers were still found only partially innervated. With additional days post-crush, nerve endings continued to differentiate into presynaptic sites and NMJs were found fully reinnervated by 12 days (**Figure 4D, 4E-F**). Importantly, there was little variability among mice denervated for the same length of time (**Figure 4E-F**), demonstrating that crushing the fibular nerve can be used as an assay to compare reinnervation of muscles between animals of the same age and sex.

The ability to faithfully compare regenerating NMJs between animals provides opportunities to understand the cellular features associated with each step required to fully repair this synapse. To examine the architecture of denervated and regenerating NMJs from the 70 days old mice used above for comparing rates of reinnervation, high-resolution confocal microscopy images of NMJs were obtained. As expected, this analysis revealed a number of changes that occur in α-motor axon nerve endings as they reinnervate muscle fibers (**Figure 4G-I**). Axonal growth cones appear to expand and begin to branch out as they contact postsynaptic sites (**Figure 4G**). These axonal branches then grow over specific regions of the postsynapse, culminating in the near complete juxtaposition of the axon nerve ending with the postsynaptic site (**Figure 4H-I**). Additional structural features in regenerating motor nerve endings that highly resemble those found during development were observed, including multiple axons competing for the same target (**Figure 4H**), culminating in only one axon innervating one muscle fiber by 12 days post-crush. Additionally, axonal branches extending beyond post-synaptic sites, referred herein as sprouts, at all stages post-injury were observed (**Figure 4I**). These sprouts were highly prevalent, even in fully innervated NMJs suggesting that the final phase of axonal repair involves retraction of extrajunctional axonal branches. Despite these obvious changes at nerve endings, post-synaptic sites remained mostly indistinguishable at all stages post-injury compared to those in uninjured muscles, including at 4 days post-crush when muscle fibers are found completely denervated. There was no obvious sign of fragmentation or significant loss and redistribution to extra-synaptic regions of AChRs. These findings strongly indicate that the fibular nerve crush method can be used as an assay to identify and test molecular, pharmacological and life-style interventions that promote repair of nerve endings at synapses, including the NMJ.

Despite recent advances, very little progress has been made in identifying muscle-derived factors required and sufficient to maintain and repair the NMJ. We therefore asked if the common fibular nerve injury method can be used to identify molecules altered at specific stages of the reinnervation process and with potential roles in repairing the NMJ. As a proof of principal, expression analysis of two NMJ-associated genes, the AChR gamma subunit and the muscle-specific kinase, MuSK[18] was performed. As demonstrated with quantitative PCR, these genes are increased following denervation and decreased as NMJs are reinnervated (**Figure 5a-b**). These genes are upregulated at 4 days post-crush, as previously reported using completely denervated muscles[19]. As nerves reinnervate muscle fibers, levels of these genes decrease and rapidly return to baseline. Among animals examined, the pattern of expression for both genes is nearly identical, demonstrating a close correlation between molecular and cellular changes at regenerating NMJs. This method therefore provides unique opportunities to identify molecular changes associated with different stages of NMJ regeneration.

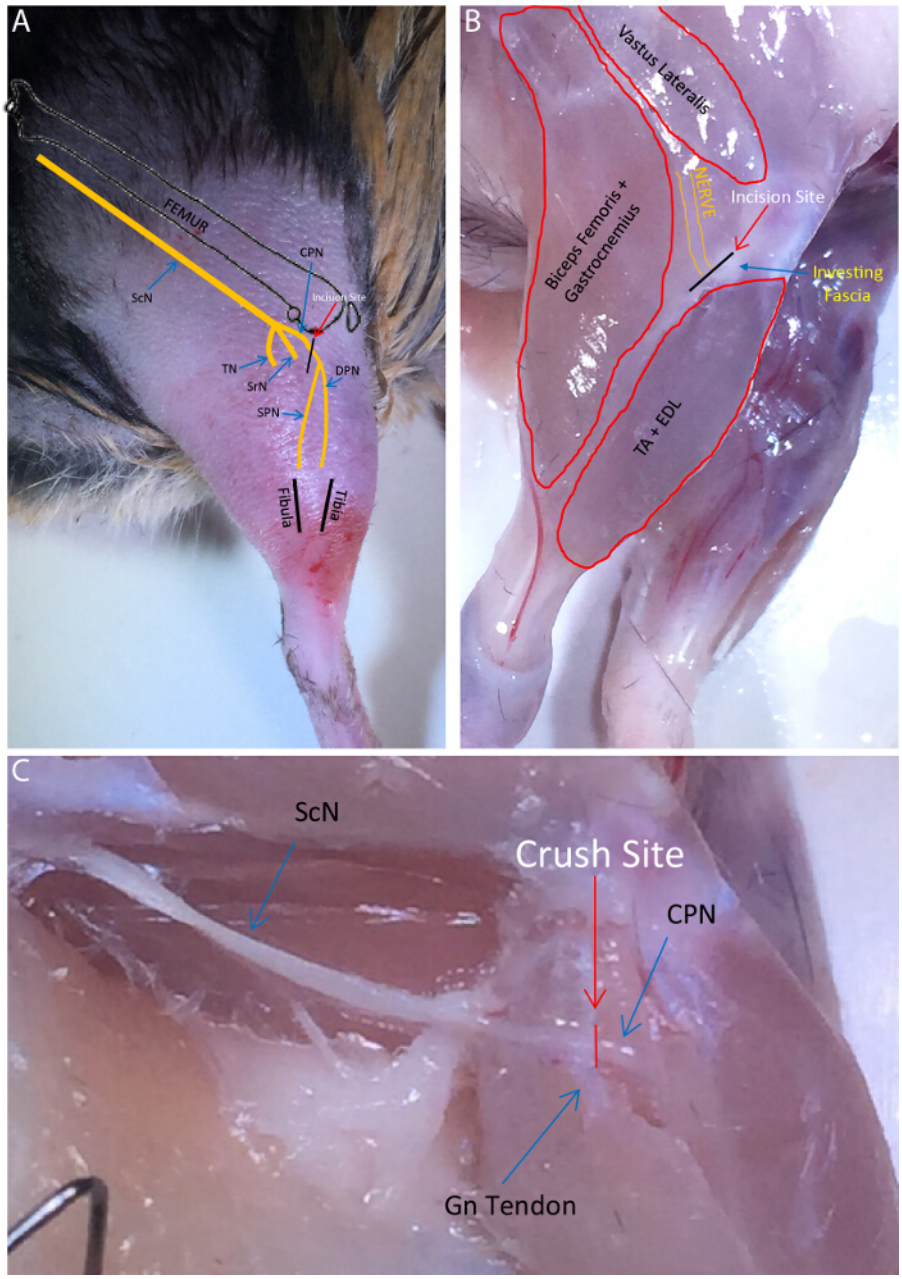

Figure 1: Common Fibular Nerve Anatomy. (**A**) Schematic detailing the course of the sciatic nerve and its terminal branches in relation to superficial and bony landmarks. ScN = Sciatic Nerve, TN = Tibial Nerve, SrN = Sural Nerve, CPN = Common Fibular Nerve, SPN = Superficial Fibular Nerve, DPN = Deep Fibular Nerve. The desired incision site is indicated. (**B**) Diagram of common fibular nerve location in relation to surrounding muscles with the skin removed. Relative incision site is shown overlying the investing fascia. TA = Tibialis Anterior Muscle EDL = Extensor Digitorum Longus Muscle. (**C**) Exposed sciatic and common fibular nerve. CPN crosses over the gastrocnemius muscle (Gn) tendon at the level of the knee. Crush site relative to tendon shown. Please click here to view a larger version of this figure.

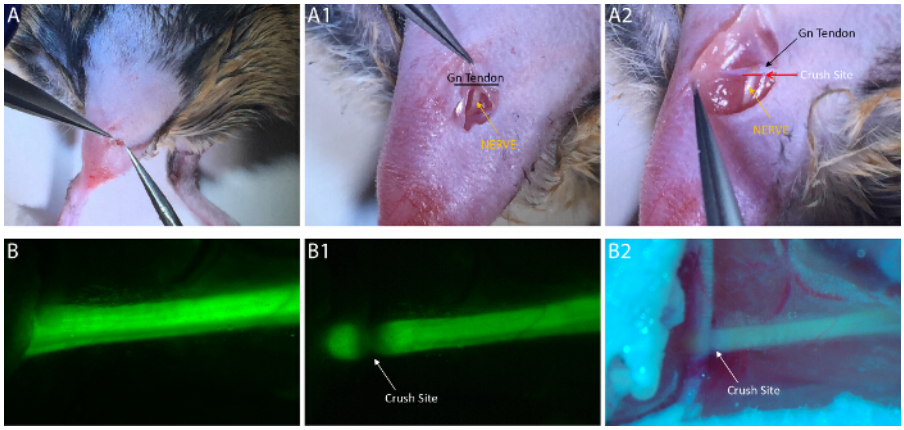

Figure 2: Common Fibular Nerve Crush Surgery. (**A**) The initial incision need only be a few cm in length. After penetrating through the skin and superficial fascia, the incision must be continued through the investing/deep fascia lying between the Biceps Femoris and TA muscles. (**A1**) The common fibular nerve is easily visualized without microscopy through the incision (Gn = Gastrocnemius Muscle). (**A2**) The intersection of the common fibular nerve and gastrocnemius tendon can be easily visualized if the incision is widened (necessary only for photographic purposes). The crush should be placed at the location marked by the red line perpendicular to the nerve and parallel to the Gn tendon. (**B**) The CPN is even more easily visualized with YFP transgenic mice under a fluorescent dissecting scope. (**B1**) The nerve loses fluorescence at the site of crush, allowing for confirmation of a full crush injury. (**B2**) A full CPN crush can still be visualized with the naked eye and room lighting. The nerve will become translucent. This image highlights the fact that the epineurium and superstructure of the CPN remain intact while simultaneously limiting damage to nearby tissue and blood vessels. Please click here to view a larger version of this figure.

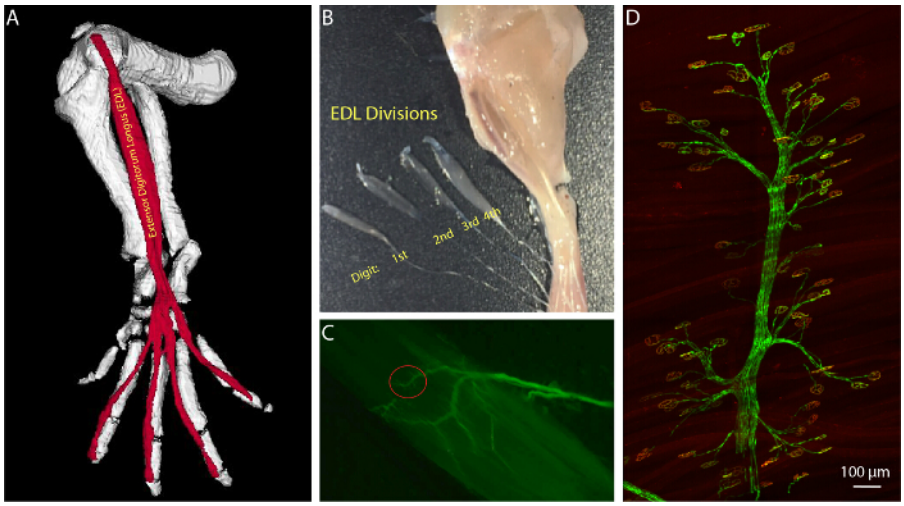

Figure 3: Anatomy of the Extensor Digitorum Longus (EDL) Muscle. (**A**) 3 dimensional image of the EDL in relation to the bones of the mouse hind limb. Generated using JAtlasView (**B**) Partially dissected EDL muscle separated into its four phalangeal divisions and marking the digits controlled by each division. (**C**) YFP labeled branch of the deep fibular nerve as it innervates the end-plate band of the EDL division controlling the second digit. (**D**) Axonal branches and their contact sites can be readily identified, allowing for consistent examination of selected NMJs. Please click here to view a larger version of this figure.

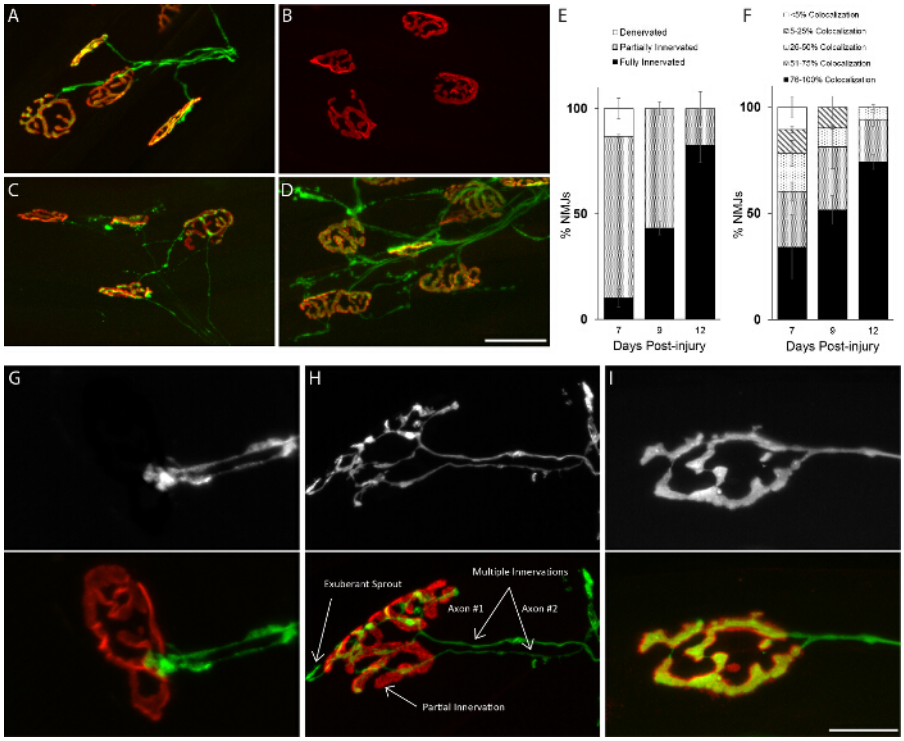

Figure 4: Similar Rates of Reinnervation Between Animals of the Same Age and Sex. Analysis of NMJs in the EDL muscle after crushing the fibular nerve. (**A**) Post-synaptic sites are completely occupied by axons in uninjured mice. (**B**) At 4 days post-crush, muscles are found completely denervated. (**C**) Axons begin to reinnervate muscles 7 days post-crush and (**D**) completely reoccupy postsynaptic sites by 12 days. (**E**-**F**) The rate of NMJ re-occupancy is nearly indistinguishable between animals denervated for the same length of time. (**G**-**I**) Representative images of re-differentiating axonal nerve endings into matured presynaptic sites. Reoccupation of postsynaptic sites follows a predictable pattern, starting with the growth cone developing branches that eventually fully occupy postsynaptic sites without extending beyond the NMJ region.Similar to development, postsynaptic sites are initially innervated by multiple re-growing axons but only one axon remains once the NMJ has completely regenerated. (**H**) Examples of exuberant axonal sprouting, partial innervation without full overlap between pre and postsynaptic apparatuses, and innervation by multiple axons indicated. 70 day-old female mice were examined; Scale Bar = 50 µm (A-D), 20 µm (G-I). Error bar = SEM. N = 3 mice. Please click here to view a larger version of this figure.

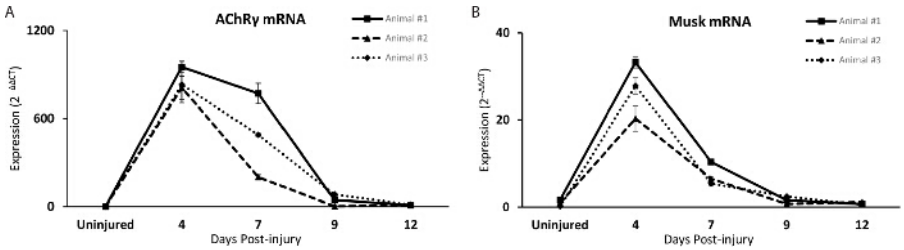

Figure 5: The Fibular Nerve Crush Method as an Assay to Identify Candidate Genes Involved in Repairing the NMJ. (**A**-**B**) The mRNA level of two NMJ-associated genes, the AChR gamma subunit and MuSK, are similarly altered in the TA muscle of mice denervated for the same length of time. With increasing time post nerve injury, levels of both transcripts decrease, returning to baseline, corroborating histological analysis showing progressive reinnervation of NMJs. Each line represents an individual mouse. Error bar = standard error of the mean of technical replicates. Please click here to view a larger version of this figure.

Discussion

The method presented in this manuscript provides unique opportunities to identify mechanisms involved in repairing neuromuscular junctions (NMJ). This method involves crushing the common fibular nerve as it passes over the gastrocnemius tendon near the knee. We show that after only 5 sec of nerve compression with a forceps, complete degeneration is noted by 4 days after injury. In young adult mice, alpha-motor axons begin to reinnervate previous synaptic sites in the extensor digitorum longus muscle (EDL) at 7 days post-injury, culminating in the reformation of presynaptic sites that are indistinguishable from those in uninjured mice by 12 days. In addition, we demonstrate that levels of select NMJ-associated molecules closely correlate with the innervation status of the NMJ. Importantly, these cellular and molecular changes are highly reproducible between animals of the same sex and age (**Figure 5a-b**), providing opportunities to identify and test factors that act to repair the NMJ. In terms of surgical procedures, the common fibular nerve branch is highly accessible as it passes over the gastrocnemius tendon, requiring only a small incision that results in little damage to surrounding muscles and vasculature.

There are a number of advantages of using the common fibular nerve to examine cellular and molecular changes associated with regenerating NMJs. The gastrocnemius tendon serves as a stable anatomical landmark to consistently injure the common fibular nerve on the same location

and distance from target muscles. This makes it possible to reliably compare the rate of regeneration of axons and reinnervation of muscles between animals of the same age and sex. The steps critical to such success include ensuring that the injury site is consistent between surgeries, full nerve crush is obtained in every animal, and minimal damage is sustained to surrounding structures. Among muscles innervated by the common fibular nerve, the tibialis anterior (TA) and extensor digitorum longus (EDL) muscles are excellent targets for assessing NMJ repair. These two muscles are primarily composed of fast type muscle fibers that are severely affected by injury, aging and diseases[5]. For NMJ analysis, the EDL muscle is particularly attractive because it can be whole-mounted to image all NMJs without distortions. It also makes it possible to correlate alterations at NMJs with changes elsewhere in muscle fibers, motor axons and surrounding cells.

The TA and EDL muscles have been extensively used to assess the impact of different molecular and lifestyle interventions on muscle and NMJ repair because of their anatomical location[20]. However, long-term denervation alters expression of genes with critical function in atrophying muscle fibers, activated immune cells and satellite cells[12-14], making it more difficult to assess cellular and molecular changes required to specifically promote regeneration of NMJs. In the method described here the fibular nerve is crushed in close proximity to the TA and EDL muscles, allowing the nerve to reach them within 7 days post-crush in young adult mice. Thus, this method should minimize loss of muscle mass and molecular changes associated with atrophying muscle fibers in the TA and EDL muscles.

The fibular nerve crush protocol can be modified in multiple distinct fashions. Nerve cut injury can readily be substituted for crush, allowing for better real-time in vivo imaging of peripheral nerve regeneration. A cut removes dead axon material as an obstacle for regrowth and ensures homogenous damage of every axon within the endoneurial tube.

When performed correctly the fibular nerve crush has few associated complications. One problem that could be encountered is failure of the nerve to reinnervate original NMJ targets. This can be caused by accidental cut injury to the nerve during surgery. Be sure to check the fine-tipped crushing forceps for any sharp edges. If at any point during surgery the quality of a nerve crush is questionable, the original incision can be widened to better visualize the nerve. While this increases the size of the wound and can damage additional structures, it can help with correctly identifying the fibular nerve and assessing whether or not a full crush was achieved.

The technique described here does possess a few limitations. First, it is mainly useful in adult mice as the structures in these animals are large enough to manipulate. Newborn and adolescent mice are much smaller, significantly increasing the difficulty of the surgery. Second, the fibular nerve contains sensory and motor axons, resulting in denervation of target tissues that may affect rates of NMJ regeneration.

The NMJ is recognized as a focal site of pathology in amyotrophic lateral sclerosis (ALS) and aging. It also has to be repaired following injury to peripheral nerves to avoid compromising motor skills and losing muscle mass. The fibular nerve crush method should aid in the identification and testing of molecules with important roles in repairing the NMJ. In one approach, this method could be used to profile mRNA and microRNA with key roles at different stages of NMJ regeneration using RNA sequence analysis. It can also be applied to selectively determine the function of candidate genes introduced and deleted from muscles. In addition, this method lends itself well to testing the ability of exogenous molecules to speed nerve and NMJ regeneration using static and live imaging.

Disclosures

The authors have nothing to disclose.

Acknowledgements

The authors thank members of the Valdez laboratory for intellectual input on experiments and comments on the manuscript.

References

1. Sanes, J. R., & Lichtman, J. W. Induction, assembly, maturation and maintenance of a postsynaptic apparatus. *Nat. Rev. Neurosci.* **2** (11), 791-805 (2001).
2. Moloney, E. B., de Winter, F., & Verhaagen, J. ALS as a distal axonopathy: molecular mechanisms affecting neuromuscular junction stability in the presymptomatic stages of the disease. *Front. Neurosci.* **8** (August), 252 (2014).
3. Apel, P. J., Alton, T., *et al.* How age impairs the response of the neuromuscular junction to nerve transection and repair: An experimental study in rats. *J Orthop Res.* **27** (3), 385-393 (2009).
4. Balice-Gordon, R. J. Age-related changes in neuromuscular innervation. *Muscle Nerve Suppl.* **5**, S83-S87 (1997).
5. Valdez, G., Tapia, J. C., Lichtman, J. W., Fox, M. A., & Sanes, J. R. Shared resistance to aging and ALS in neuromuscular junctions of specific muscles. *PloS one.* **7** (4), e34640 (2012).
6. Nguyen, Q. T., Sanes, J. R., & Lichtman, J. W. Pre-existing pathways promote precise projection patterns. *Nat. Neurosci.* **5** (9), 861-867 (2002).
7. Küry, P., Stoll, G., & Müller, H. W. Molecular mechanisms of cellular interactions in peripheral nerve regeneration. *Curr Opin Neurol.* **14** (5), 635-639 (2001).
8. Gaudet, A. D., Popovich, P. G., & Ramer, M. S. Wallerian degeneration: gaining perspective on inflammatory events after peripheral nerve injury. *J Neuroinflammation.* **8**, 110 (2011).
9. Chen, P., Piao, X., & Bonaldo, P. Role of macrophages in Wallerian degeneration and axonal regeneration after peripheral nerve injury. *Acta Neuropathol.* **130** (5), 605-618 (2015).
10. Chen, Z.-L., Yu, W.-M., & Strickland, S. Peripheral regeneration. *Annu Rev Neurosci.* **30**, 209-233 (2007).
11. Darabid, H., Perez-Gonzalez, A. P., & Robitaille, R. Neuromuscular synaptogenesis: coordinating partners with multiple functions. *Nat. Rev. Neurosci.* **15** (11), 703-718, (2014).
12. Geuna, S. The sciatic nerve injury model in pre-clinical research. *J. Neurosci. Methods.* **243**, 39-46 (2015).

13. Batt, J. A. E., & Bain, J. R. Tibial nerve transection - a standardized model for denervation-induced skeletal muscle atrophy in mice. *J. Vis. Exp.* (81), e50657 (2013).
14. Savastano, L. E., Laurito, S. R., Fitt, M. R., Rasmussen, J. A., Gonzalez Polo, V., & Patterson, S. I. Sciatic nerve injury: a simple and subtle model for investigating many aspects of nervous system damage and recovery. *J. Neurosci. Methods.* **227**, 166-180 (2014).
15. Kang, H., & Lichtman, J. W. Motor axon regeneration and muscle reinnervation in young adult and aged animals. *J Neurosci.* **33** (50), 19480-19491 (2013).
16. Gage, G. J., Kipke, D. R., & Shain, W. Whole animal perfusion fixation for rodents. *J. Vis. Exp.* (65), e3564 (2012).
17. Feng, G., Mellor, R. H., *et al.* Imaging Neuronal Subsets in Transgenic Mice Expressing Multiple Spectral Variants of GFP. *Neuron.* **28** (1), 41-51 (2000).
18. Sanes, J. R., & Lichtman, J. W. Development of the vertebrate neuromuscular junction. *Annu Rev Neurosci.* **22**, 389-442 (1999).
19. Bowen, D. C., Park, J. S., *et al.* Localization and regulation of MuSK at the neuromuscular junction. *Dev Biol.* **199** (2), 309-319 (1998).
20. Gay, S., Jublanc, E., Bonnieu, A., & Bacou, F. Myostatin deficiency is associated with an increase in number of total axons and motor axons innervating mouse tibialis anterior muscle. *Muscle Nerve.* **45** (5), 698-704 (2012).
21. Livak, K. J., & Schmittgen, T. D. Analysis of relative gene expression data using real-time quantitative PCR and the 2(-Delta Delta C(T)) Method. *Methods.* (San Diego, Calif.) **25** (4), 402-408 (2001).

